Int J Adv Manuf Technol (2010) 49:111–121
DOI 10.1007/s00170-009-2368-1

ORIGINAL ARTICLE

An experimental investigation on friction stir welding of AZ31B magnesium alloy

G. Padmanaban · V. Balasubramanian

Received: 16 July 2008 / Accepted: 12 October 2009 / Published online: 28 October 2009
© Springer-Verlag London Limited 2009

Abstract The conventional fusion welding of magnesium alloys often produces porosity in the weld joint, which deteriorates its mechanical properties. To solve this problem, friction stir welding (FSW), a solid-state welding technique, can be applied for joining of magnesium alloys. In this investigation, an attempt was made to understand the effect of FSW process parameters such as tool rotational speed, welding speed, and axial force on tensile properties of AZ31B magnesium alloy. Fourteen joints were fabricated using different levels of tool rotational speed, welding speed, and axial force. Tensile properties of the welded joints were evaluated and correlated with the weld zone microstructure and hardness. From this investigation, it is found that the joints fabricated using a tool rotational speed of 1,600 rpm, a welding speed of 0.67 mm/s, and an axial force of 3 kN yielded superior tensile properties compared to other joints. Optimum level of heat generation, formation of finer grains, and higher hardness are the main reasons for the superior tensile properties of these joints. Fatigue properties of FSW joints were evaluated, and it was found that fatigue properties of FSW joints were slightly lower than the base metal.

Keywords Magnesium alloy · Friction stir welding · Tool rotational speed · Welding speed · Axial force · Tensile properties · Fatigue properties

G. Padmanaban · V. Balasubramanian (✉)
Centre for Materials Joining & Research (CEMAJOR),
Department of Manufacturing Engineering, Annamalai University,
Annamalai Nagar 608002, India
e-mail: visvabalu@yahoo.com

G. Padmanaban
e-mail: gknaban@rediffmail.com

1 Introduction

Magnesium alloys are potential candidates to replace aluminium alloys in many structural applications owing to some of their unique properties. Magnesium alloys exhibit low density, high strength to weight ratio, and good castability. These alloys have attracted the interest of modern manufacturing such as the automobile, computer, communication, and consumer electronic appliances industries [1]. They are also considered as advanced materials in terms of energy conservation and environmental pollution regulations. However, the joining of magnesium alloy parts, which may be crucial for the above applications, is still limited [2].

Conventional fusion welding methods for joining magnesium alloys produce some defects such as porosity and hot crack, which deteriorate their mechanical properties. The production of the defect-free weld requires complete elimination of the surface oxide layer and selection of suitable welding parameters. Magnesium alloys are currently welded using techniques such as gas tungsten arc welding (GTAW) and gas metal arc welding (GMAW); while reasonable welding speeds can be achieved, problems can be experienced such as high welding residual stresses and changes in microstructure resulting from melting and solidification. High purity shielding gases are necessary to prevent weld contamination; magnesium alloys can readily oxidize in the weld zone because of their high-chemical reactivity at high temperatures [3]. Friction stir welding (FSW) is capable of joining magnesium alloys without melting, and thus, it can eliminate problems related to solidification. As FSW does not require any filler material, the metallurgical problems associated with it can also be eliminated, and good quality weld can be obtained [4].

Table 1 Chemical composition (weight percentage) of base metal AZ31B magnesium alloy

Al	Mn	Zn	Mg
3.0	0.20	1.0	Balance

Even though the process offers many advantages, very limited numbers of investigations were carried out so far on FSW of magnesium alloys. Grain growth and lower hardness in the FSW zone of AZ31B-H24 magnesium alloy were reported by Lee et al. [5]. Wang et al. [6] observed grain refinement and higher microhardness in FSW zone of AZ31 magnesium alloy. Esparza et al. [7] found a recrystallized and equiaxed grain structure in the FSW zone of AZ31B magnesium alloy. The relationship between material flow and defects during friction stir welding of AZ31 magnesium alloy was reported by Zhang et al. [8]. The influence of different ratios of rotational speed/traverse speed on mechanical properties of different zones of friction stir welded AZ31 magnesium alloy was studied by Abbasi Gharacheh et al. [9]. They found that increasing the aforementioned ratio leads to a slight decrease in yield and ultimate strength of the stir zone and the transitional zone. It was also observed that increasing rotational/traverse speed ratio increases the weld nugget size and decreases the incomplete root penetration. Pareek et al. [10] investigated the microstructural changes due to friction stir welding of AZ31B-H24 magnesium alloy and analysed their effect on mechanical properties and corrosion behaviour of the joints. They found that the mean grain size across all weld samples was coarser than the mean grain size of the as-received magnesium alloy samples. The effect of welding speed on the material flow patterns was studied by Zhang Hua et al. [11]. They suggested that there are two main material flows in the nugget, one is from the advancing side (flow 1), and the other is from the retreating side; flow 1 decides whether the weld is defect-free or not. Cao et al. [12] investigated the influence of welding speed on joint quality of friction stir welded AZ31B-H24 magnesium alloy. They concluded that the hardness decreased gradually from the base metal through the heat-affected zone to the thermomechanically affected zone and then to the stir zone where the lowest hardness was obtained. Higher welding speed produced slightly higher hardness in the stir zone.

The load carrying capacity of welded joints is generally evaluated by tensile strength of the joints. The tensile strength is controlled by the microstructure and hardness of the weldment. The microstructure and hardness of the weldment are influenced by the weld thermal cycle. The weld thermal cycle is influenced by the welding process parameters. However, there is no systematic investigation reported so far to study the effect of FSW process parameters, especially tool rotational speed, welding speed, and axial force on tensile properties of AZ31B magnesium alloy and fatigue properties of friction stir welded AZ31B magnesium alloy joints. Hence, the present investigation was carried out to study the effect of FSW process parameters on tensile properties of AZ31B magnesium alloy joints and evaluate the fatigue properties of friction stir welded AZ31B magnesium alloy joints fabricated at optimised condition.

2 Experimental work

The rolled plates of 6-mm-thick AZ31B magnesium alloy were cut into the required size (220×75 mm) by machining process. Square butt joint configuration was prepared to fabricate FSW joints. The initial joint configuration was obtained by securing the plates in position using mechanical clamps. The direction of welding was normal to the rolling direction. Single-pass welding procedure was used to fabricate the joints. Nonconsumable tool made of high carbon steel with threaded pin profile was used to fabricate the joints. The chemical composition and mechanical properties of base metal are presented in Tables 1 and 2. The optical and scanning electron microscopic (SEM) micrographs of base metal are shown in Fig. 1, and it basically contains coarse grains along with appreciable amount of subgrains (Fig. 1a). Figure 1b shows SEM image of base metal. It contains coarser grains with $Al_{12}Mg_{17}$ intermetallic compounds. The $Al_{12}Mg_{17}$ intermetallic compounds are quite coarse, and the distribution is nonuniform in the base metal.

The tool nomenclature and process parameters used to fabricate the joints are presented in Table 3. An indigenously designed and developed FSW machine (15 hp; 3,000 rpm; 25 kN) was used to fabricate the joints. In total, 14 joints were fabricated using different combination of process parameters (Table 4).

The welded joints were sliced and then machined to the required dimension, according to the American Society for Testing and Materials (ASTM) E8M-04 standard for sheet

Table 2 Mechanical properties of base metal AZ31B magnesium alloy

Yield strength (MPa)	Ultimate tensile strength (MPa)	Elongation (%)	Reduction in cross-sectional area (%)	Notch tensile strength (MPa)	Notch strength ratio (NSR)	Hardness (Hv)
171	215	14.7	14.3	192	0.89	69.3

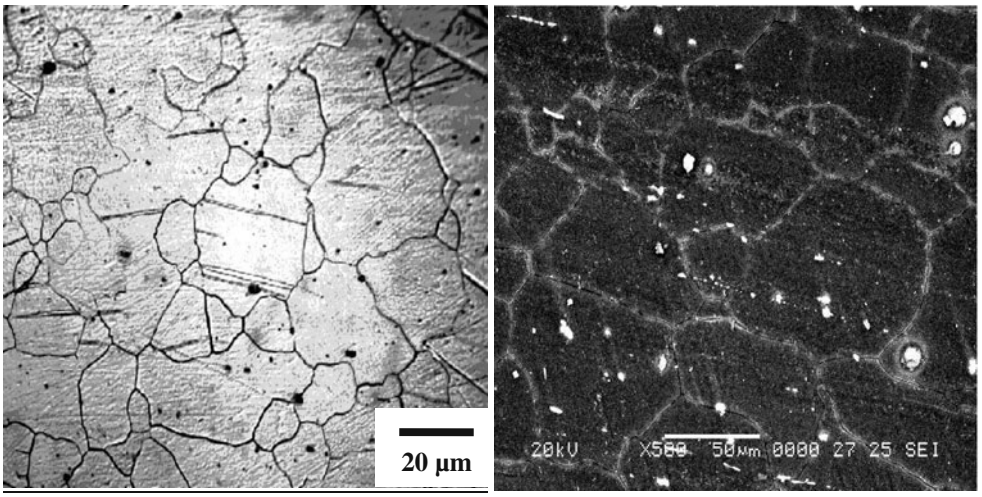

Fig. 1 Optical and SEM micrographs of base metal

(a) OM **(b) SEM**

type material (i.e., 50 mm gauge length and 12.5 mm gauge width). Two different tensile specimens were prepared to evaluate the transverse tensile properties of the welded joints. The smooth (unnotched) tensile specimens were prepared to evaluate yield strength, tensile strength, and elongation of the joints. Notched specimens were prepared to evaluate notch tensile strength and notch strength ratio of the weld. Tensile test was carried out in a 100-kN electromechanical-controlled universal testing machine (maker: FIE-Bluestar, India; model: UNITEK-94100). The 0.2% offset yield strength was derived from the load-displacement diagram. The percentage of elongation was also evaluated, and the values are presented in Tables 5, 6 and 7. Vicker's microhardness testing machine (maker: SHIMADZU, Japan; model: HMV-2 T) was employed for measuring the hardness across the weld cross section with 0.05 kg load for 20 s.

The S–N curve of the friction stir welded AZ31B magnesium alloy joint, fabricated using optimised process parameter, was obtained by using a servohydraulic-controlled (maker: INSTRON; model: 8801) 100-kN capacity fatigue testing machine with a frequency of 10 Hz under constant amplitude loading (R=stress ratio=$\sigma_{min}/\sigma_{max}$=0.1). Fatigue experiment was conducted at five different stress levels (50, 75, 100, 125, and 150 MPa) for smooth specimen and five different stress levels for (30, 40, 50, 60, and 70 MPa) for notched specimen. Hourglass-type (smooth) specimens were prepared from FSW joints to evaluate the fatigue life (S–N behaviour). Notched specimens were also prepared from FSW joints to evaluate the fatigue notch factor and notch sensitivity factor. Procedures prescribed by the ASTM E 466-96 (reapproved 2002) standard were followed for the preparation of the specimens.

The specimens for metallographic examination were sectioned to the required size and then polished using different grades of emery papers. A standard reagent made of 4.2 g picric acid, 10 ml acetic acid, 10 ml diluted water, and 70 ml ethanol was used to reveal the microstructure of the welded joints. Microstructural analysis was carried out using a light optical microscope (maker: MEIJI, Japan; model: MIL-7100) incorporated with an image analysing software (Metal Vision) and scanning electron microscope (maker: JOEL, Japan; model: 5610 LV). Energy-dispersive spectrum (EDS) analysis was carried out using scanning

Table 3 FSW process parameters and tool nomenclature

Tool rotational speed (rpm)	1,000, 1,200, 1,400, 1,600, 1,800, 2,000
Welding speed (mm/s)	0.37, 0.67, 1.25, 1.76, 2.25
Axial force (kN)	2, 3, 4
Pin length, L (mm)	5.7
Tool shoulder diameter, D (mm)	18
Pin diameter, d (mm)	6
D/d ratio of tool	3.0
Tool inclined angle (deg)	0
Shoulder deepness inserted into the surface of base metal (mm)	0.2
Pitch (mm) and included angle (deg) of Threaded pin	1 and 60
Hardness of the tool (Rc)	70
Chemical composition of the tool (wt%)	C 0.75, Si 0.25, Mn 0.32

Table 4 FSW process parameters used to fabricate the joints

Joint number	Rotational speed (rpm)	Welding speed (mm/s)	Axial force (kN)	Heat input[a] (kJ/mm)
1	1,000	0.67	3	0.34
2	1,200	0.67	3	0.41
3	1,400	0.67	3	0.47
4	1,600	0.67	3	0.54
5	1,800	0.67	3	0.60
6	2,000	0.67	3	0.68
7	1,600	0.37	3	0.98
8	1,600	0.67	3	0.54
9	1,600	1.25	3	0.29
10	1,600	1.76	3	0.21
11	1,600	2.25	3	0.16
12	1,600	0.67	2	0.36
13	1,600	0.67	3	0.54
14	1,600	0.67	4	0.72

[a] The heat input for friction stir welding process was calculated using the following expression [21] $q = \frac{2\pi}{3S} \times \mu \times p \times \omega \times Rs \times \eta$

where:

μ coefficient of friction

p normal force in kN

ω rotational speed in rev/s

Rs shoulder radius in m

S welding speed in mm/s

electron microscope (maker: JOEL; model: 5610LV) at high magnification to estimate the weight percentage of elements.

3 Results

3.1 Tensile properties

The transverse tensile properties such as yield strength, tensile strength, percentage of elongation, percentage of reduction in cross-sectional area, notch tensile strength, notch strength ratio, and joint efficiency of friction stir welded AZ31B magnesium alloy joints were evaluated. In each condition, three specimens were tested, and the average of three results is presented in Tables 5, 6 and 7. Of the fourteen joints fabricated, the joint fabricated with a rotational speed of 1,600 rpm, welding speed of 0.67 mm/s, and axial force of 3 kN exhibited higher yield strength (166 MPa), tensile strength (208 MPa), elongation (7.3%), and reduction in cross sectional area (5.5%).

Notch strength ratio is the ratio between the tensile strength of notched specimen at maximum load to ultimate tensile strength of unnotched specimen. Notch strength ratio (NSR) is found to be less than unity (<1) for all the joints. This suggests that the AZ31B magnesium alloy is sensitive to notches, and they fall in to the "notch brittle materials" category. The NSR is 0.89 for unwelded parent metal, and FSW causes reduction in NSR of the weld metal. The joint fabricated with a rotational speed of 1,600 rpm, welding speed of 0.67 mm/s, and axial force of 3 kN exhibited higher notch strength ratio (0.77), which is 14% lower compared to unwelded parent metal.

Joint efficiency is a ratio between tensile strength of welded joint and tensile strength of unwelded parent metal. The joint fabricated with a rotational speed of 1,600 rpm, welding speed of 0.67 mm/s, and axial force of 3 kN exhibited a maximum joint efficiency of 96.7%.

3.2 Microhardness and microstructure

The hardness was measured across the weld using Vicker's microhardness testing machine, and the values are presented in Figs. 2, 3, and 4. The hardness of base metal (unwelded parent metal) is 69.3 Hv. Vicker's microhardness is measured along the midthickness line of cross section of the joint. The joints fabricated with the rotational speed of 1,600 rpm, welding speed of 0.67 mm/s, axial force of 3 kN recorded higher hardness (78 Hv) in the stir zone, and this is also one of the reasons for superior tensile properties of these joints compared to other joints. There are two main reasons for the improved hardness of stir zone. Firstly, since

Table 5 Effect of rotational speed on transverse tensile properties (welding speed=0.67 mm/s; axial force=3 kN)

Joint number	Rotational speed (rpm)	Yield strength (MPa)	Ultimate tensile strength (MPa)	Elongation in 50mm gauge length (%)	Reduction in cross - sectional area (%)	Notch tensile strength (MPa)	Notch strength ratio	Joint efficiency (%)
1	1,000	149	187	4.0	3.8	137	0.72	87.0
2	1,200	153	191	5.0	4.0	144	0.75	88.8
3	1,400	162	202	5.3	4.6	153	0.76	94.0
4	1,600	166	208	7.3	5.5	160	0.77	96.7
5	1,800	164	205	6.0	5.0	148	0.72	95.3
6	2,000	162	203	5.9	4.7	143	0.70	94.4

Table 6 Effect of welding speed on transverse tensile properties (rotational speed=1,600 rpm; axial force=3 kN)

Joint number	Welding speed (mm/s)	Yield strength (MPa)	Ultimate tensile strength (MPa)	Elongation in 50mm gauge length (%)	Reduction in cross-sectional area (%)	Notch tensile strength (MPa)	Notch strength ratio	Joint efficiency (%)
7	0.37	152	190	2	2.4	141	0.73	88.6
8	0.67	166	208	7.3	5.5	160	0.77	96.7
9	1.25	163	204	5.3	5.1	154	0.75	94.8
10	1.76	163	204	5.3	5.1	152	0.74	94.8
11	2.25	160	200	4.6	4.9	142	0.71	93.1

the grain size of stir zone is much finer than that of base metal, grain refinement plays an important role in material strengthening. Secondly, the small particles of intermetallic compounds are also a benefit to hardness improvement [6]. All the joints were nondestructively inspected using ultrasonic testing, and no defect was detected in the joint, indicating that the sound joint was achieved. The location of failure in all the tensile specimen was invariably at the thermomechanically affected zone (TMAZ) region on the advancing side (Fig. 5), which is consistent with the lowest hardness distribution in the TMAZ of advancing side.

The optical micrographs taken at FSW zone of all the joints are displayed in Figs. 6, 7, and 8. From the micrographs, it is understood that there is an appreciable variation in average grain diameter of weld region in AZ31B magnesium alloy. Due to FSW, the coarse grains of base metal are changed in to fine grains in the weld region. The joints fabricated with a rotational speed of 1,600 rpm, welding speed of 0.67 mm/s, and axial force of 3 kN contain finer grains in the weld region compared to other joints. This is also one of the reasons for higher tensile properties of these joints compared to other joints. To identify, the reason for failure in TMAZ region, the detailed microstructural analysis was carried out across the joint, and the micrographs are displayed in Figs. 6, 7, and 8. From the micrographs, it is inferred that there is an appreciable variation in grain size (average grain diameter) across the weld. The grain size of TMAZ is larger than the nugget region, and this is because of insufficient plastic flow and thermal exposure [6]. Grains are relatively smaller in the retreating side of TMAZ compared to advancing side, and this is caused by the greater straining in this location. The similar observation was made by Pareek et al. [10] in friction stir welding of AZ31B magnesium alloy. This may be another reason for failure along the TMAZ region on the advancing side. SEM micrograph of stir zone is shown in Fig. 9. It reveals that the stir zone contains finer grains with significantly refined $Al_{12}Mg_{17}$ intermetallic compounds which are homogeneously distributed in the magnesium matrix. During FSW process, magnesium grains plastically deform with rotation of the tool, but the second phase, which is a brittle phase, is hard to deform. This causes stress concentration on the second phase. When applied stress is higher than the fracture strength of the second phase, fracture takes place, and large second phases change into smaller ones gradually. The EDS analysis indicated that the intermetallic compounds in both base metal and stir zone are $Al_{12}Mg_{17}$. The similar result was observed by Wang et al. [6] in friction stir welding of AZ31B magnesium alloy.

Transmission electron microscopic (TEM) micrographs of base metal and FSW joint are shown in Fig. 10. From the TEM micrographs, it is found that the FSW joint contains finer magnesium grains with finer $Al_{12}Mg_{17}$ precipitates as compared to base metal. The dislocation density is lower as compared to base metal. SEM fractographs of fractured tensile specimens of as-received and friction stir welded AZ31B magnesium alloy are shown in Fig. 11. The base metal exhibits elongated dimples and friction stir welded joint exhibits finer dimples on the fractured surface.

3.3 Fatigue properties

Two types of fatigue test specimens such as (1) unnotched specimens and (2) notched specimens were prepared to

Table 7 Effect of axial force on transverse tensile properties (rotational speed=1,600 rpm; welding speed=0.67 mm/s)

Joint number	Axial force (kN)	Yield strength (MPa)	Ultimate tensile strength (MPa)	Elongation in 50mm gauge length (%)	Reduction in cross - sectional area (%)	Notch tensile strength (MPa)	Notch strength ratio	Joint efficiency (%)
12	2	160	200	6.8	5.2	151	0.75	93
13	3	166	208	7.3	5.5	160	0.77	96.7
14	4	158	198	6.5	4.9	147	0.73	92.1

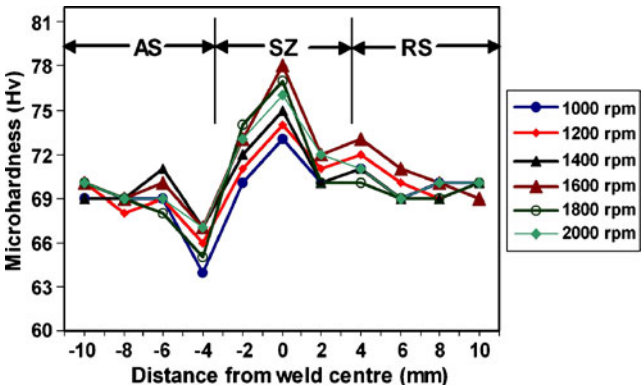

Fig. 2 Effect of rotational speed on hardness

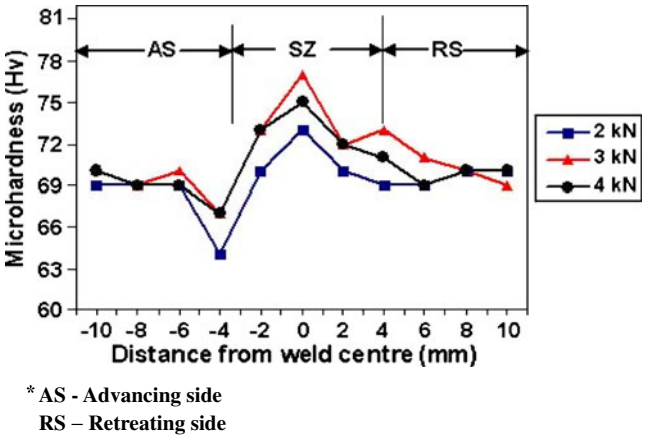

Fig. 4 Effect of axial force on hardness

evaluate the effect of notches on fatigue behaviour. The fatigue testing experiments were conducted at different stress levels, and all the experiments were conducted under uniaxial tensile loading condition using servohydraulic fatigue testing machine. From FSW joint, five specimens were tested, and the test results are used to plot S–N curves. Figure 12 shows the fatigue life of unnotched and notched specimens in the form of S–N curves.

The S–N curve in the high cycle fatigue region is represented by the Basquin equation [13]:

$$S^n N = A \tag{1}$$

where S is the stress amplitude, N is the number of cycles to failure, and n and A are empirical constants. Each S–N curves shown in Fig. 12 can be represented by the above equation. From those equations, the empirical constants n (slope of the curve) and A (intercept of the curve) have been evaluated, and they are presented in Table 8.

The effect of notches on fatigue strength is determined by comparing the S–N curves of notched and unnotched specimens. The data for notched specimens are usually plotted in terms of nominal stress based on the net section of the specimen. The effectiveness of the notch in decreasing the fatigue limit is expressed by the fatigue strength reduction factor or fatigue notch factor, K_f. The fatigue notch factor for FSW joints has been evaluated using the following expression [14], and they are given in Table 8.

$$K_f = \text{Fatigue limit of unnotched specimen} / \text{Fatigue limit of notched specimen} \tag{2}$$

The notch sensitivity of a material in fatigue is expressed by a notch sensitivity factor q, and it can be evaluated using the following expression [15]:

$$q = (K_f - 1)/(K_t - 1) \tag{3}$$

where K_t is the theoretical stress concentration factor and is the ratio of maximum stress to nominal stress. Using the above expression, fatigue notch sensitivity factor q has been evaluated for FSW joints, and they are presented in Table 8.

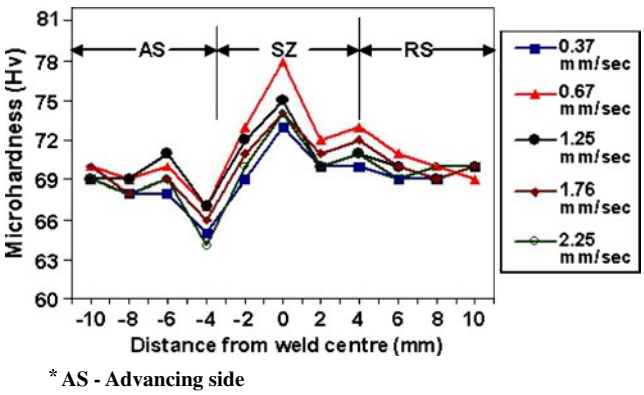

Fig. 3 Effect of welding speed on hardness

4 Discussion

The ultimate requirement for a FSW process is to create a certain amount of friction heat, which can keep the welding material in a well-plasticised state with a suitable temperature, and to generate a high hydrostatic pressure along the joint line so that a sound weld can be generated. The heat generation in FSW is in direct proportion to deformation and frictional energy created during the stirring process. The latter depends on the friction factor and friction area between the tool shoulder and work piece surface, as well on the rotation speed of the welding head pin and the pressure applied to the welding tool head shoulder [16]. The heat input in the weld area is affected by welding conditions like rotational speed, welding speed, and axial force. Generally, more frictional heat input is generated at a

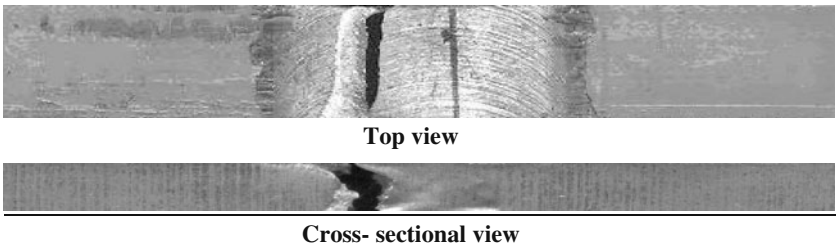

Fig. 5 Failure location in welded joint during tensile test

lower welding speed, higher rotational speed, and at higher axial force relative to opposite case.

Intense plastic deformation and frictional heating during FSW resulted in the generation of fine recrystallized grains. During dynamic recrystallization, either decreasing the temperature or raising the strain rate will produce a finer grain structure. In this investigation, relatively finer magnesium grain structure is produced by FSW [6].

The tensile properties of the joints made with different welding conditions resulted in lowest tensile strength and ductility at lowest spindle speed (1,000 rpm) for a given welding speed (0.67 mm/s). As the spindle speed increased (1,600 rpm), both the strength and elongation improved, reaching maximum before falling again at high rotational speeds (2,000 rpm). Higher tool rotational speed usually results in higher temperature and slower cooling rate in the FSW zone. A higher rotational speed also causes excessive release of stirred materials to the upper surface, which resultantly produces microvoids in the FSW zone, and this is one of the reasons for lower tensile properties of the joints. Lower heat input condition due to lower rotational speed results in lack of stirring, and this is one of the reasons for lower tensile properties of the joints. [17]. Of the six joints fabricated using six different tool rotational speeds, the joint fabricated at a rotational speed of 1,600 rpm exhibited superior tensile properties, and this is due to optimum heat generation under this condition.

Higher welding speed results in lower heat input per unit length of the weld, causes lack of stirring in the friction stir processing zone, which leads to lower tensile properties of the joints. Lower welding speed results in higher temperature, and slower cooling rate in the weld zone causes grain growth, which subsequently leads to lower tensile properties of the joints [18]. Of the five joints fabricated using five welding speeds, the joint fabricated at a welding speed of 0.67 mm/s exhibited superior tensile properties, and this is also due to optimum heat generation under this condition.

Heat is generated by the rotating tool under the application of axial force, and this heat is the primary source for welding. This temperature at top portion of the

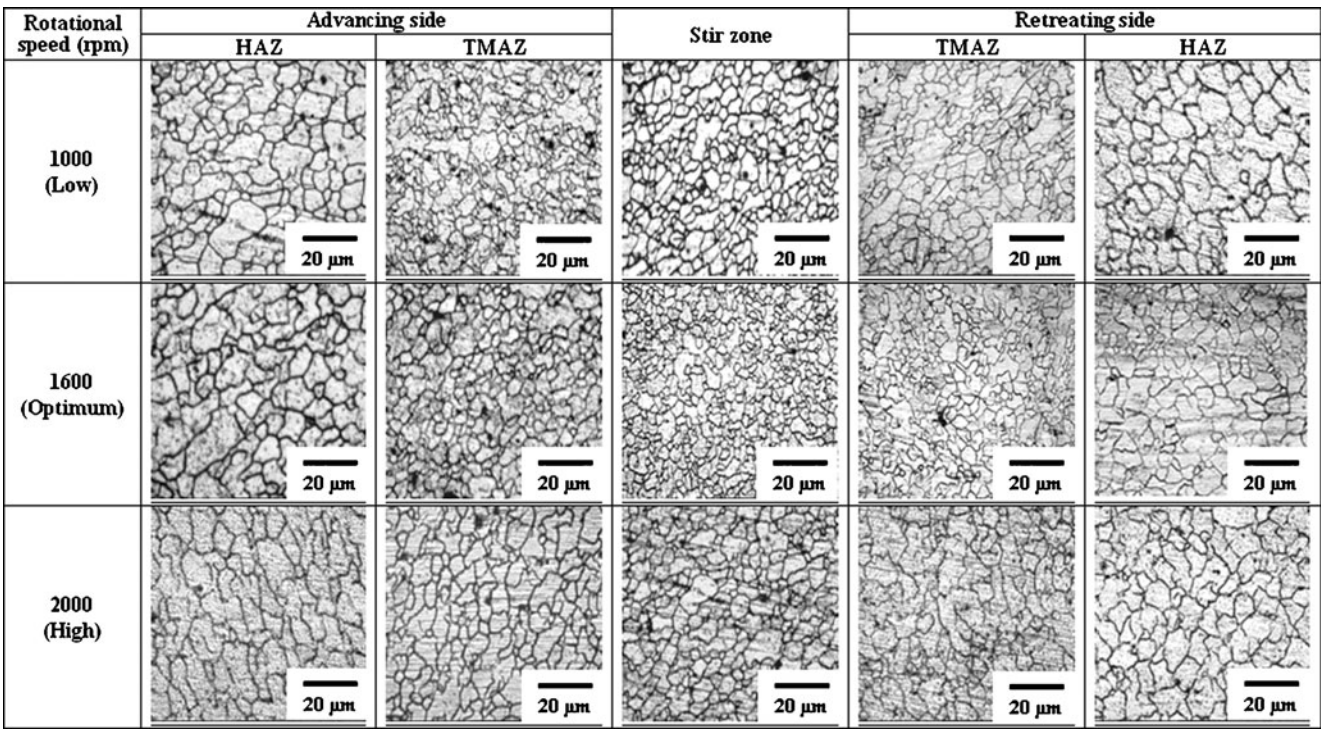

Fig. 6 Effect of rotational speed on microstructure

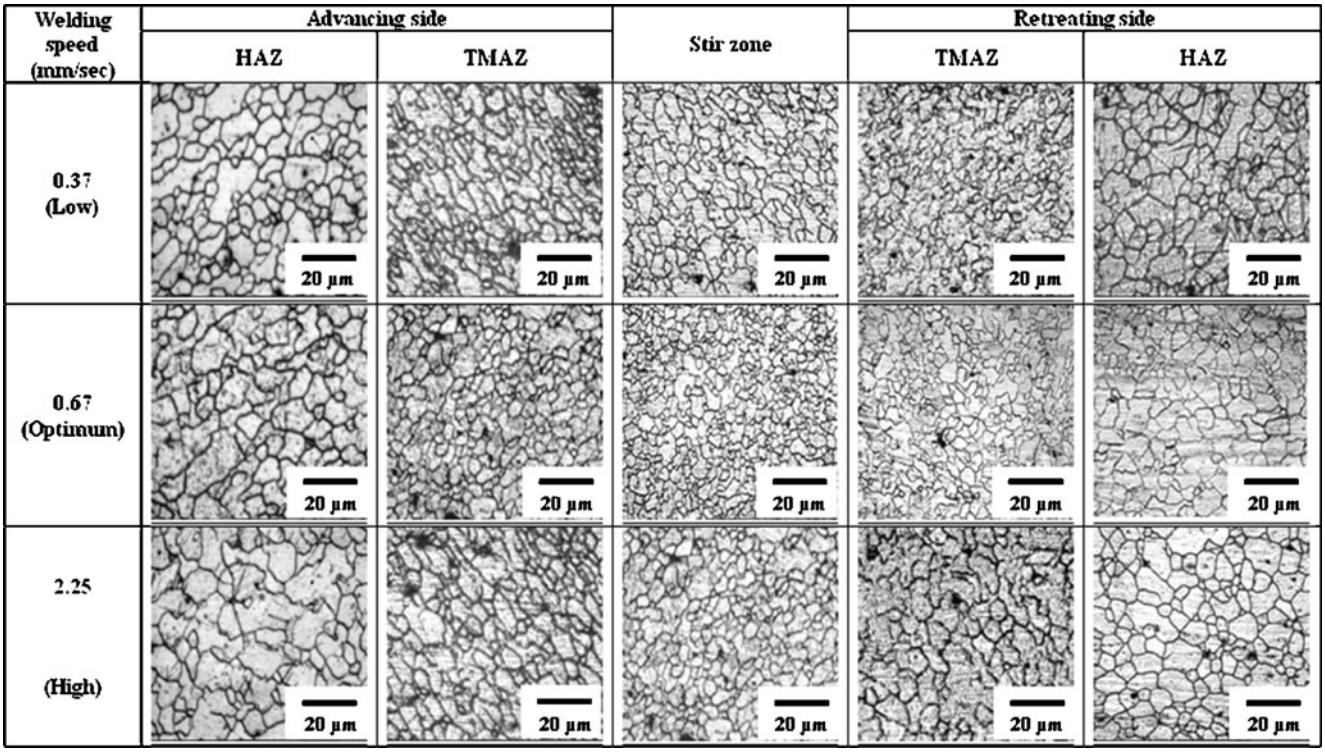

Fig. 7 Effect of welding speed on microstructure

V-shaped nugget clearly indicated that the major heat source originated through the frictional heat generated by shoulder of the tool by the application of axial force. Due to high temperature at the top portion caused by higher axial force, nugget zone is widened near the top of the surface because of the close contact between the tool shoulder and the upper surface of the plates to be joined [19]. The axial force is directly responsible for the plunge depth of the tool

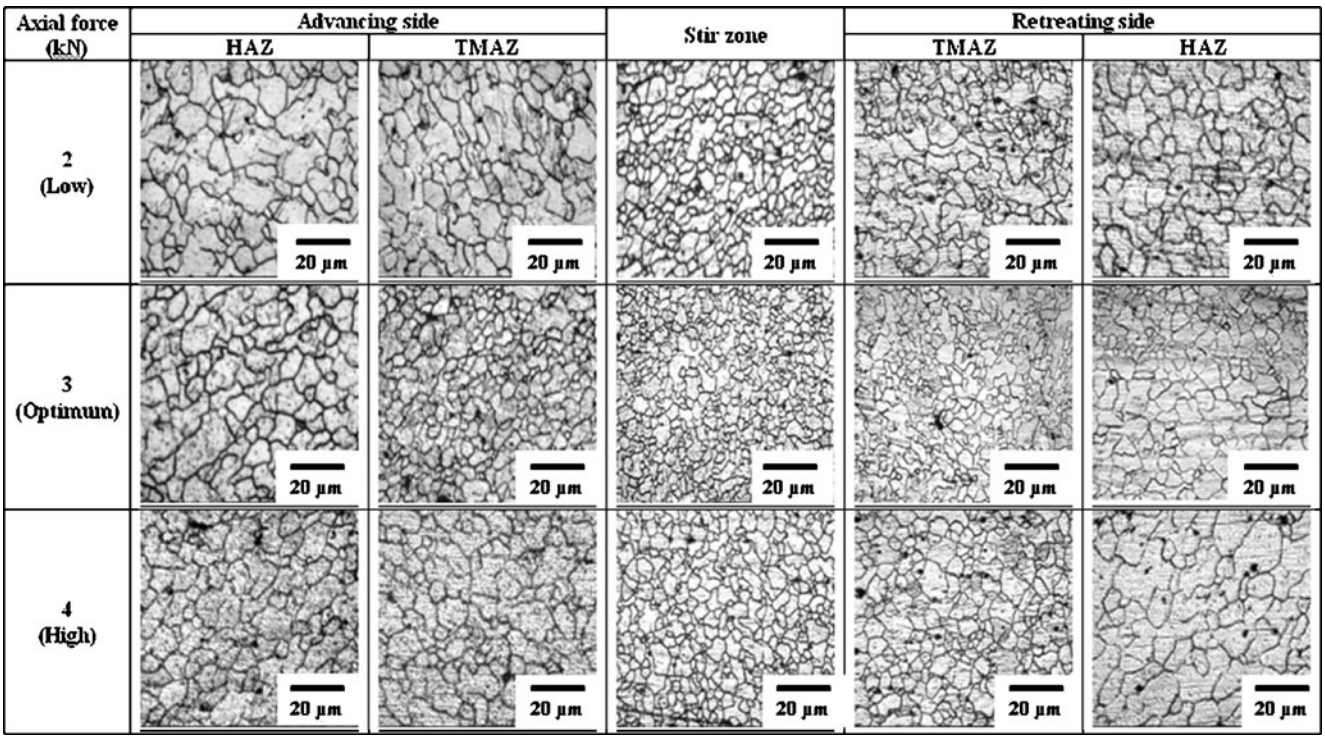

Fig. 8 Effect of axial force on microstructure

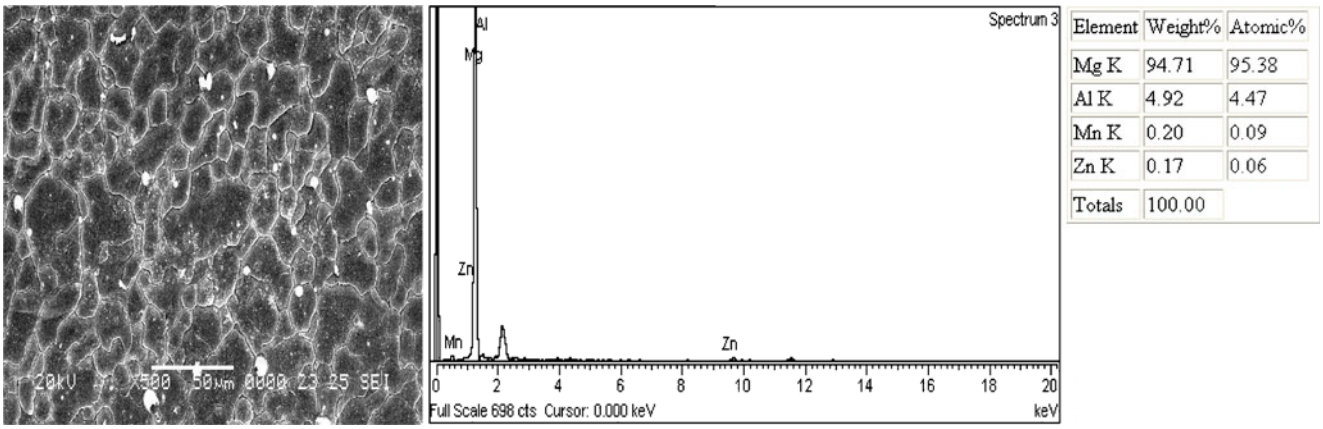

(a) SEM micrograph of stir zone **(b) EDS result at the stir zone**

Fig. 9 SEM micrograph and EDS results of optimised joint

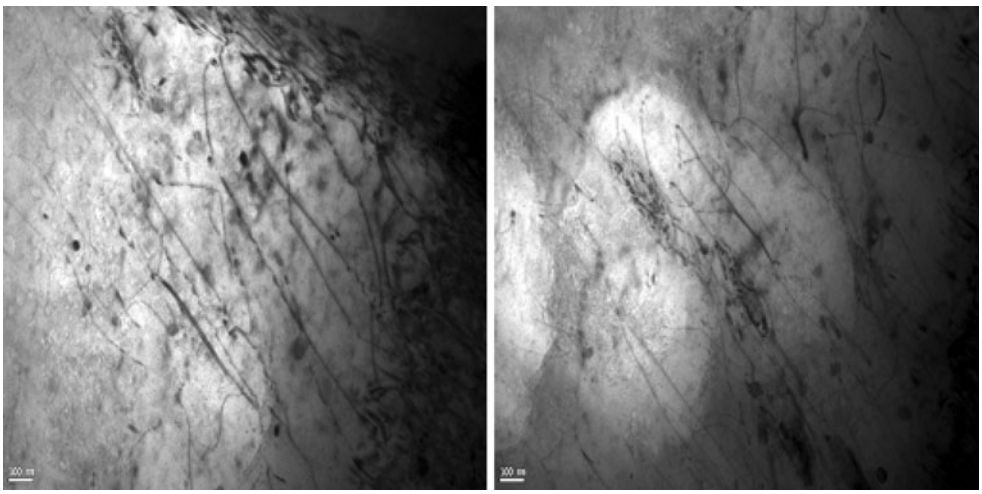

(a) Base metal **(b) FSW joint**

Fig. 10 TEM Micrographs of optimised joint

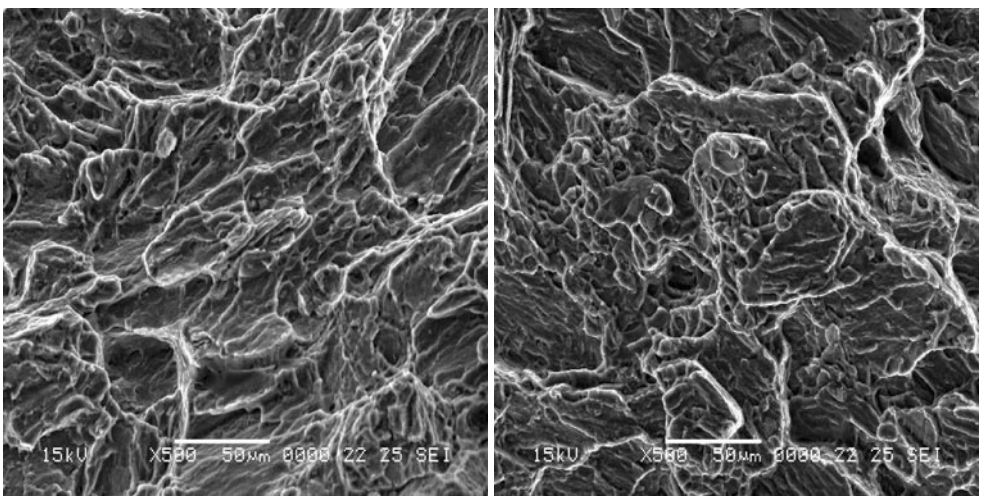

(a) Base metal **(b) FSW joint**

Fig. 11 SEM Fractographs of base metal and FSW joint

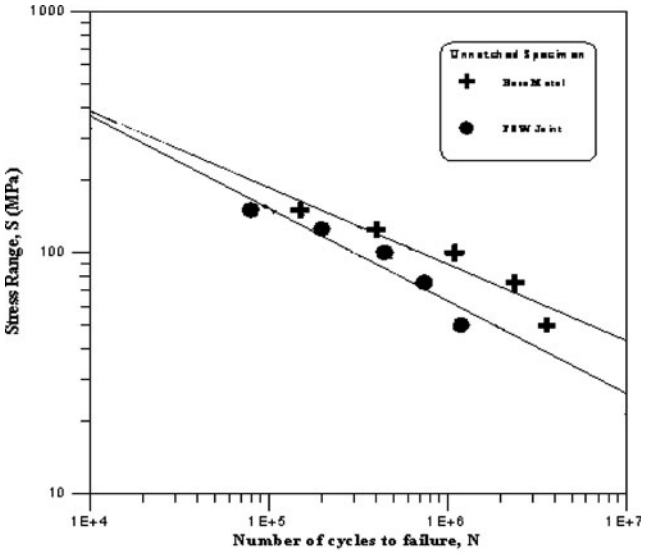

(a) S-N curves for unnotched (smooth) specimen

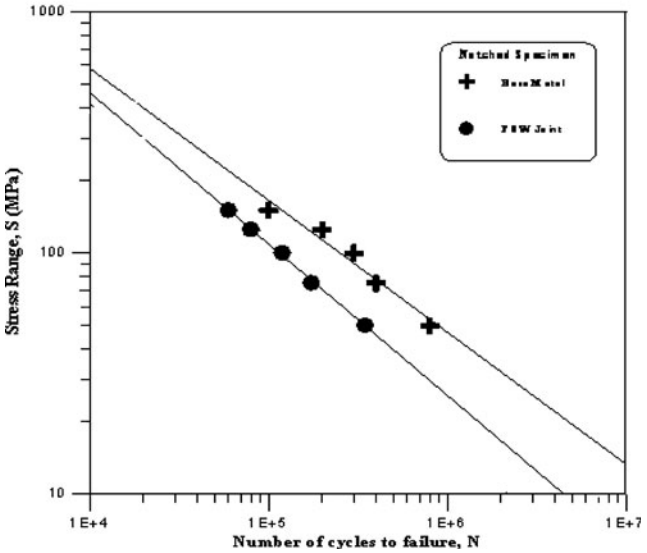

(b) S-N curves for notched specimen

Fig. 12 Effect of friction stir welding on S–N behaviour

pin into the workpiece and load characteristics associated with linear friction stir weld. When the axial force is relatively low, there is a possibility of insufficient stirring (less mechanical working) at the bottom. While with higher axial force, the weld is sound with full penetration. It shows that sufficient axial force is required to form good weld. This is because the temperature during friction stir welding defining the amount of plasticised metal, and the temperature is greatly dependent on the axial force [20]. Of the three joints fabricated using three levels of axial force, the joint fabricated at an axial force of 3 kN exhibited superior tensile properties, and this is also due to optimum heat generation under this condition.

The fatigue strength of unwelded AZ31B magnesium alloy is 72 MPa. But the fatigue strength of FSW joint is 51 MPa. This indicates that there is a 29% reduction in fatigue strength values due to friction stir welding. Similar trend has been observed in notched specimens also. The introduction of notch will alter the stress distribution at the vicinity of notch, the stress value will be magnified nearer to the tip of the notch, and this will have a definite effect on fatigue life of the components. The fatigue notch factor of unwelded AZ31B magnesium alloy is 2.25. But the fatigue notch factor of FSW joint is 2.72. This indicates that there is an 18% increase in fatigue notch factor value due to friction stir welding. Generally, if the fatigue notch factor is lower, then the fatigue life of the joints will be higher and vice versa. Similar trend has been observed in notch sensitivity factor values also since it is derived using fatigue notch factor values.

Slope of the S–N curve is another measure to understand the fatigue performance of welded joints. If the slope of the S–N curve is larger, then the fatigue life will be higher and vice versa. The unwelded parent metal shows highest slope, the FSW joint shows lowest slope, and it is clearly understood from Fig. 12.

5 Conclusions

In this investigation, an attempt was made to study the effect of FSW process parameters on tensile properties of friction stir welded AZ31B magnesium alloy. From this investigation, the following important conclusions are derived:

1. AZ31B magnesium alloy was successfully joined without any macrolevel defects by friction stir welding process under the following range of process parameters: tool rotational speed of 1,000–2,000 rpm,

Table 8 Fatigue properties of friction stir welded AZ31B magnesium alloy joints

Joint type	Slope of the S–N curve (n)	Intercept of the S–N curve (A)	Fatigue limit of unnotched specimens at 2×10^6 cycles (MPa)	Fatigue limit of notch specimens at 2×10^6 cycles (MPa)	Fatigue notch factor (K_f)	Notch sensitivity factor (q)
Base metal	−0.32	7,176	72	32	2.25	0.051
FSW	−0.38	12,629	51	18	2.72	0.070

welding speed of 0.37–2.25 mm/s, and axial force of 2–4 kN.

2. Moreover, the joint fabricated with the rotational speed of 1,600 rpm, welding speed of 0.67 mm/s, and axial force of 3 kN showed higher tensile properties, compared to their counterparts.
3. The above welding parameters could have generated optimum heat that is exactly sufficient to cause the material to flow plastically without excess or inadequate mechanical working. This is the main reason for the formation of finer grains in the weld region and subsequently led to higher tensile strength.

Acknowledgements The authors are grateful to the Department of Manufacturing Engineering, Annamalai University, Annamalai Nagar, India for extending the facilities of Material Testing Laboratory to carry out this investigation. The authors wish to place their sincere thanks to Science and Engineering Research Council (SERC), Department of Science and Technology (DST), New Delhi for financial support rendered through a R&D project no. SR/S3/MERC-062/2004.

References

1. Mordike BL, Ebert T (2001) Magnesium—properties, applications. Potential Mater Sci Eng A 302:37–45
2. Munitz A, Cotler C, Stern A, Kohn G (2001) Mechanical properties and microstructure of gas tungsten arc welded magnesium AZ91D plates. Mater Sci Eng A 302:68–73
3. Magnesium and magnesium alloy (1999) ASM Specialty Hand book, ASM International, pp 194–199
4. Afrin N, Chen DL, Cao X, Jahazi M (2008) Microstructure and tensile properties of friction stir welded AZ31B magnesium alloy. Mater Sci Eng A 472:179–186
5. Lee WB, Yeon YM, Jung SB (2003) Joint properties of friction stir welded AZ31B–H24 magnesium alloy. Mater Sci Techno 19:785–790
6. Wang XH, Wang KS (2006) Microstructure and properties of friction stir butt-welded AZ31 magnesium alloy. Mater Sci Eng A 431:114–117
7. Esparza JA, Davis WC, Trillo EA, Murr LE (2002) Friction stir welding of magnesium alloy AZ31B. J Mater Sci Lett 21:917
8. Zhang H, Lin SB, Feng JC, Ma ShL (2006) Defects formation procedure and mathematic model for defect free friction stir welding of magnesium alloy. Mater Des 27:805–809
9. Abbasi Gharacheh M, Kokabi AH, Daneshi GH, Shalchi B, Sarrafi R (2006) The influence of the ratio of "rotational speed/traverse speed" (ω/v) on mechanical properties of AZ31 friction stir welds. Int J Mach Tool Manu 46:1983–1987
10. Pareek M, Polar A, Rumiche F, Indacochea JE (2007) Metallurgical evaluation of AZ31B–H24 magnesium alloy friction stir welds. Mater Eng Perform 16(5):655–662
11. Hua Z, Huiqiang WU, Jihua H, Sanbao WN, Lin WU (2007) Effect of welding speed on the material flow patterns in friction stir welding of AZ31 magnesium alloy. Rare Met 26:158–162
12. Cao X, Jahazi M (2008) Effect of welding speed on the quality of friction stir welded butt joints of a magnesium alloy. Mater Des. doi:10.1016/j.matdes.2008.08.040
13. Dieter GE (1988) Mechanical metallurgy. Tata McGraw Hill, New York
14. Sonsino CM (1999) Fatigue assessment of welded joints in Al-Mg-4.5 Mn aluminium alloy AA 5083 by local approaches. Inter J Fat 21:985–999
15. Courtney TH (2000) Mechanical behaviour of materials, 4th edn. McGraw Hill, New York
16. Buffa G, Hua J, Shivpuri R, Fratini L (2006) Design of the friction stir welding tool using the continuum based FEM model. Mater Sci Eng A 419:389–396
17. Lee WB (2004) Mechanical properties related to microstructural variation of 6061 al alloy joints by friction stir welding. Mater Trans 45(5):1700–1705
18. Lee WB, Yeon YM, Jung S-B (2003) The joint properties of dissimilar formed Al alloys by friction stir welding according to the fixed location of materials. Script Mater 49:423–428
19. Fonda RW, Lambrakos SG (2002) Analysis of friction stir welds using an inverse problem approach. Sci Tech Weld Join 7(3):177–181
20. Zhang HW, Zhang Z, Chen JT (2005) The finite element simulation of the friction stir welding process. Metall and Mater Trans A 403:305–316
21. Heurtier P, Jones MJ, Desrayaud C, Driver JH, Montheillet F, Allehaux D (2006) Mechanical and thermal modelling of friction stir welding. J Mater Process Technol 171:348–357